

Application of a Novel Halogen-Free Intumescent Flame Retardant for Acrylonitrile-Butadiene-Styrene

Liu Yi, Yi JiangSong, Cai XuFu

Department of Polymer Science and Engineering, Sichuan University, Chengdu 610065, China

Received 24 April 2011; accepted 26 June 2011

DOI 10.1002/app.35153

Published online 18 October 2011 in Wiley Online Library (wileyonlinelibrary.com).

ABSTRACT: A novel intumescent flame retardant (IFR), containing ammonium polyphosphate (APP) and poly(tetramethylene terephthalamide) (PA4T), was prepared to flame-retard acrylonitrile-butadiene-styrene (ABS). The flame retardation of the IFR/ABS composite was characterized by limiting oxygen index (LOI) and UL-94 test. Thermogravimetric analysis (TGA) and TGA coupled with Fourier transform infrared spectroscopy (TG-FTIR) were carried out to study the thermal degradation behavior of the composite and look for the mechanism of the flame-retarded action. The morphology of the char obtained after combustion of the composite was studied by scanning electron microscopy (SEM). It has been found the intumescent flame retardant showed good flame retardancy, with the LOI value of the PA4T/APP/ABS (7.5/22.5/70) system

increasing from 18.5 to 30% and passing UL-94 V-1 rating. Meanwhile, the TGA and TG-FTIR work indicated that PA4T could be effective as a carbonization agent and there was some reaction between PA4T and APP, leading to some crosslinked and high temperature stable material formed, which probably effectively promoted the flame retardancy of ABS. Moreover, it was revealed that uniform and compact intumescent char layer was formed after combustion of the intumescent flame-retarded ABS composite. © 2011 Wiley Periodicals, Inc. *J Appl Polym Sci* 124: 1475–1482, 2012

Key words: acrylonitrile-butadiene-styrene; intumescent flame retardant; ammonium polyphosphate; TGA; TG-FTIR

INTRODUCTION

Acrylonitrile-butadiene-styrene (ABS) is a kind of widely used thermoplastic copolymer due to its attractive properties such as good processability, chemical resistance, and low cost.^{1–5} However, the easy flammability restricts its many applications.^{6,7} Traditionally, bromine-containing compounds such as decabromodiphenyl oxide (DBDPO), 1,2-bis(2,4,6-tribromophenoxy)ethane (BTBPOE), and tetrabromobisphenol (TBBPA), etc., were regarded as very good flame retardants for ABS resin.⁸ However, regarding the environmental protection, the application of these halogen-containing flame retardants has been limited because they will generate great quantities of toxic and corrosive fumes during combustion. Consequently, to develop a nonhalogenated flame-retardant system becomes an attractive and emergent subject. The halogen-free flame retardants commonly used include aluminum hydroxide and magnesium hydroxide, phosphorus-containing compounds, and phosphorus-nitrogen-containing compounds.⁹ How-

ever, high loadings of them are needed to obtain a good flame retardant level, which destroy physical and mechanical properties of the polymer composites obviously.^{10–12}

In recent years, intumescent flame retardant (IFR) additives have received great attention. It involves the formation on heating of a swollen multicellular thermally stable char insulating the underlying material from the flame action.¹³ A typical IFR system is the mixture of three ingredients, namely, a carbon source—a carbonization agent, an acid source—a carbonization catalyst, and a gas source—a blowing agent. On heating, IFR can form a foamed cellular charred layer on the surface of the material, which can act as a barrier between fire and polymer, and then results in the extinguishment of combustion to protect the underlying materials.¹⁴ Among of those IFR ingredients, the commonly used carbonization catalyst is ammonium polyphosphate (APP). It can react with the carbonization agents such as pentaerythritol (PER), mannitol or sorbitol, to generate the char.^{15,16} But these polyol kind carbonization agents are confronted with the problems of exudation and water solubility. Besides, they are not compatible with the polymeric matrix, which weaken the mechanical properties of the material. Thus, lots of attention has been focused on the application of different carbonization agents. Recently, it was found that polyamide could also act as carbonization agent

Correspondence to: C. XuFu (caixf2004@sina.com).

Contract grant sponsor: National Natural Sciences Foundation of China; contract grant number: 50973066.

in intumescent flame retardant, such as PA6, PA66, PA11.^{17–20} Levchik SV et al.¹⁷ have demonstrated that PA6 could be used as carbonization agent, and PA6/APP mixture led to flame retardancy properties of interest, by developing an intumescent charred shield. It was also found a chemical interaction taking place between APP and PA6 on heating, resulting in destabilization of PA-6 and modification of its degradation to form some crosslinking chemical structure to strengthen the char layer. In addition, Yuan Liu et al.²⁰ adopted another polyamide, PA11, as charring agent to flame-retard PP, in combination with PER and APP. It was found PA11 showed not only good charring ability, but also good compatibility with polymeric matrix.

In this work, a novel intumescent flame retardant, containing poly(tetramethylene terephthalamide) (PA4T) as carbonization agent and APP as acid source and blowing agent, was prepared to intumescent flame-retard ABS. Flammability and thermal stability of the novel IFR/ABS system have been investigated.

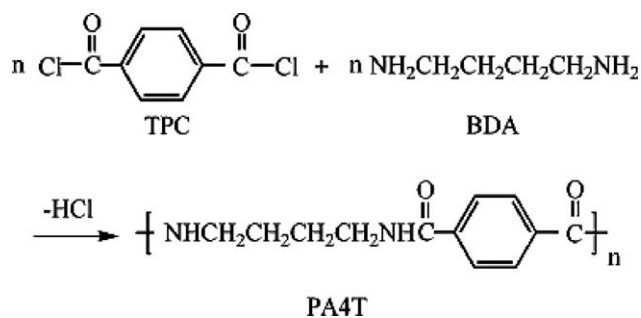
EXPERIMENTAL

Materials

Acrylonitrile-butadiene-styrene (ABS) copolymer (0215-A) was supplied by Jilin Petrochemical (Jilin, China). Ammonium polyphosphate (APP) was obtained from Zhejiang Longyou GD Chemical Industry Corp. (Longyou, China). Pentaerythrite (PER) was purchased Damao Chemical Reagent Corp. (Tianjin, China). Poly(tetramethylene terephthalamide) (PA4T) was synthesized and its preparation is described in section Synthesis of PA4T. All materials used in synthesizing PA4T including terephthaloyl chloride (TPC), 1,4-butanediamine (BDA), triethylamine (TEA), calcium chloride (CaCl_2), and *n*-methyl-pyrrolidone (NMP) were purchased from Kelong Chemical Reagent Corp. (Chengdu, China).

Synthesis of PA4T

A 150-mL three-necked round bottom flask equipped with a stirrer was charged with 3 g CaCl_2 , 9.1 g TEA (as acid adsorbent), 3.97 g BDA (0.45 mol/L), and 100 mL NMP. The mixture was stirred. When the mixture dissolved completely, the flask was cooled to 0–5°C. After that, 9.14 g TPC (0.45 mol/L) was added slowly to the flask within about 0.5 h, during which the reaction temperature was still kept at 0–5°C. Then the flask was heated up to 30°C and the reaction would be completed after 2 h. After that, the reaction mixture was cooled to room temperature, and then the mixture was poured into distilled water and filtered. The obtained white solid



Scheme 1 Synthesis of PA4T.

was washed with hot water about 80°C and dried in a vacuum at 100°C to constant weight (Product yield: 76%). The synthesis route was illustrated in Scheme 1.

Preparation of flame-retardant ABS samples

ABS, APP, PA4T were dried in vacuum at 100°C for 24 h before use. ABS resins with different APP, PA4T content were prepared via a twin screw extruder ($D = 25$ mm, $L/D = 33$, TSSJ - 25, Chengguang, China) with screw rotating rate of 100 rpm, and the barrel setting temperatures were 200, 215, 220, 220, 230, and 230°C. Then the extruded composites, dried at 100°C for 12 h, were injected into standard testing bars at 220–230°C for the tests of combustibility, using an injection-molding machine (PS40E5ASE, Nissei Plastic Industrial).

Measurements

Structural characterization of PA4T

IR spectroscopy was applied with a Nicolet IS10 FTIR spectrometer using KBr pellets. $^1\text{H-NMR}$ (400Hz) spectra was recorded on a FT-80A NMR by using CF_3COOD as a solvent.

LOI and UL-94 tests

LOI data of all samples was obtained at room temperature on an oxygen index instrument (XYC-75) produced by Chende Jinjian Analysis Instrument Factory, according to GB/T 2406-93 standard. The dimensions of all samples were $130 \times 6.5 \times 3$ mm³. Vertical burning rates (UL-94) of all samples were measured on a CZF-2 instrument produced by Jiangning Analysis Instrument Factory, with sample dimensions of $130 \times 13 \times 3$ mm³, according to ASTM D3801.

Thermogravimetric analysis (TGA) and TG-FTIR analysis

Thermogravimetric analysis (TGA) was performed on a thermal analyzer (TGA/DSC 1 Mettler/Toledo)

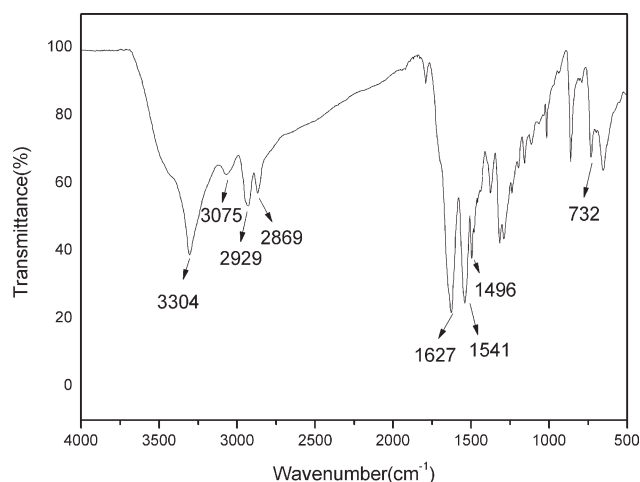


Figure 1 The FTIR spectrum of PA4T.

at a heating rate of 10°C/min. 5–10 mg of the sample was examined under pure nitrogen at a flowing rate of 50 mL/min from 50 to 800°C.

TGA coupled with Fourier transform infrared spectroscopy (TG-FTIR) consisted of a TGA/DSC 1 (Mettler/Toledo) coupled with a IS10 FTIR spectrometer (Nicolet), at a heating rate of 10°C/min. Totally, 5–10 mg of the sample was examined under pure nitrogen at a flowing rate of 50 mL/min from 50 to 800°C.

Fourier transform infrared spectrum (FTIR) of the residual char formed during thermal degradation was obtained with a Nicolet IS10 FTIR spectrometer using KBr pellet.

Scanning electron microscopy analysis

The surface morphology of the char obtained after the LOI test was observed by using a HITACHI X-650 scanning electron microscope (SEM). The specimens were previously coated with a conductive gold layer.

RESULTS AND DISCUSSION

Characterization of PA4T

Figure 1 presents the FTIR spectrum of the synthesized PA4T. The absorption bands at 3075 cm^{-1} , 1496 cm^{-1} correspond to the benzene ring, and the peaks at 2929 cm^{-1} , 2869 cm^{-1} are assigned to asymmetric and symmetric stretching absorption of $-\text{CH}_2-$. The absorptions at 1627 cm^{-1} and 1541 cm^{-1} are attributed to amide I (stretching mode of $\text{C}=\text{O}$) and amide II (flexural vibration of $-\text{NH}$), respectively. Absorption at 3304 cm^{-1} is assigned to the stretching mood of $-\text{NH}$.

The ^1H -NMR spectrum of the synthesized PA4T is shown in Figure 2. As can be seen, the peak at 7.7 ppm is

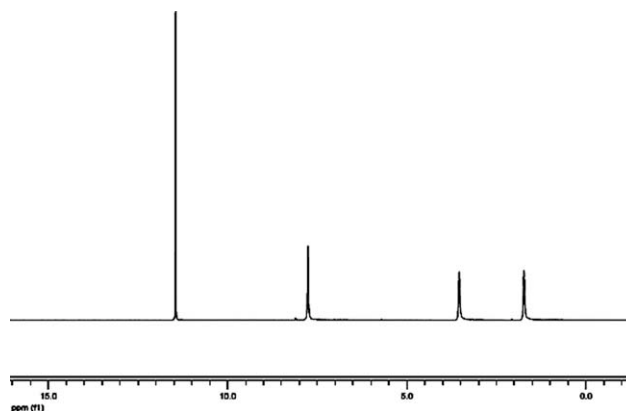


Figure 2 The ^1H -NMR spectrum of PA4T.

assigned to the proton of benzene ring. The peaks at 3.5 ppm and 1.7 ppm are attributed to two types of $-\text{CH}_2-$ protons, namely $-\text{N}-\text{CH}_2-\text{C}'-\text{C}-\text{CH}_2-\text{C}'-$ the former corresponding to the $-\text{CH}_2-$ protons adjacent to the amide group. All the information above confirms that the target product is synthesized successfully.

Flammability

In our research, a novel IFR was produced to flame-retard ABS, containing APP (as acid source and blowing agent) and PA4T (as carbonization agent). And a series of IFR with different weight ratio of PA4T to APP were compounded with ABS. Table I gives the LOI values and UL-94 rate of the IFR/ABS systems at 30% additive level. It can be found, ABS is an easily flammable polymeric material with its LOI value only 18.5 and when the addition of APP was 30%, LOI value of the APP/ABS system increased to 25, but still failed in UL-94 test. However, when APP was mixed with PA4T and incorporated into ABS, LOI values of the IFR/ABS systems increased continuously, along with the increasing addition of PA4T. When the weight ratio of PA4T to APP increased to 1 : 3, that is, PA4T was 7.5% and APP was 22.5%, the IFR/ABS system showed the best flame retardancy with its LOI value reaching the maximum of 30. However, when the ratio of

TABLE I
Effect of IFR on Flame Retardancy of IFR/ABS System

Sample	Components (%)				Flame retardancy	
	ABS	APP	PA4T	PER	LOI(%)	UL-94
1	100	0	0	0	18.5	Burning
2	70	30	0	0	25	Burning
3	70	15	15	0	26.5	Burning
4	70	20	10	0	29	V-1
5	70	22.5	7.5	0	30	V-1
6	70	24	6	0	28	Burning
7	70	25	5	0	27	Burning
8	70	22.5	0	7.5	27	V-0

TABLE II
Effect of IFR Addition on Flame Retardancy of IFR/ABS System (PA4T:APP=1 : 3)

Sample	Components (%)		Flame retardancy	
	ABS	IFR	LOI(%)	UL-94
9	80	20	26	burning
10	75	25	27	burning
11	70	30	30	V-1
12	65	35	31	V-1
13	60	40	32	V-0

PA4T to APP continued to increase, LOI values of the IFR/ABS systems decreased. In addition, when the weight ratio of PA4T to APP was between 1 : 2 and 1 : 3, the IFR/ABS systems reached V-1 rating during the UL-94 test. In addition, the flammability of the conventional PER/APP/ABS (7.5/22.5/70) system was also given in Table I. Its UL-94 rating was V-0, but the LOI value was only 27. So, it could be concluded the novel PA4T/APP/ABS system could almost lead to equal flame retardancy than the conventional system.

Table II shows the influence of IFR addition on flame retardancy of IFR/ABS system, setting the ratio of PA4T to APP as 1 : 3. It was found, LOI values of the IFR/ABS system increased with the increase of IFR loading. LOI value of IFR/ABS system was 26% with the addition of the 20% IFR. However, when the addition of the IFR increased to 40%, the LOI value reached to 32% and passed the UL-94 V-0 rating. This experimental result above demonstrated that this new IFR is very effective in flame-retarding ABS.

Thermal stability and mechanism of flame-retarded action

The thermal degradation behaviors of the IFR/ABS systems were investigated by TGA in pure nitrogen.

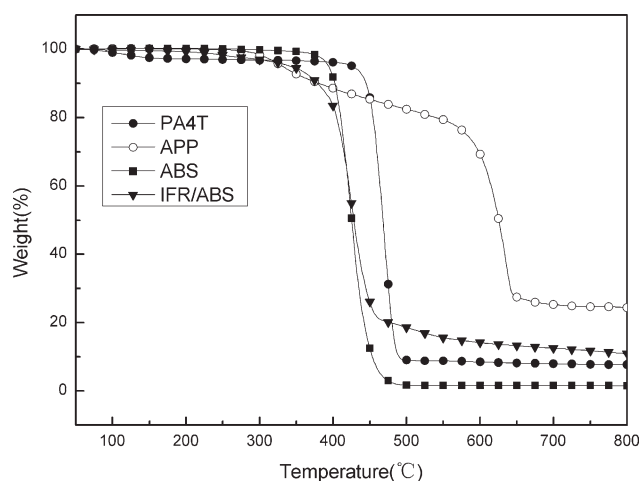


Figure 3 TG curves of IFR/ABS system.

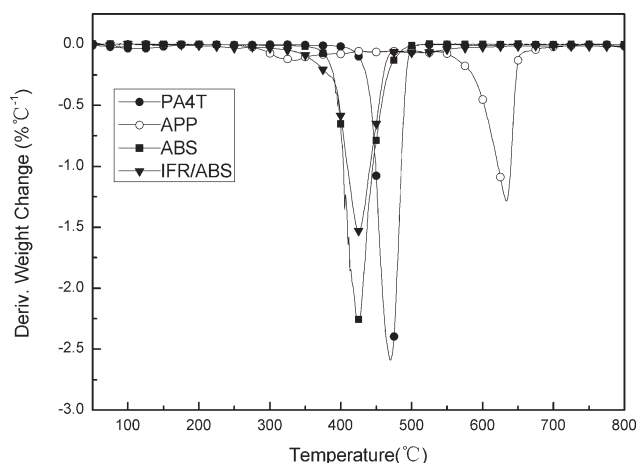


Figure 4 DTG curves of IFR/ABS system.

Figures 3 and 4 show the TG and DTG curves of the IFR/ABS system and its components, main data collected from these curves is shown in Table III. It could be found from Figures 3 and 4 and Table III, the initial decomposition temperature of ABS is 394°C, based upon 5% weight loss. The thermal degradation process of ABS only have one step with the main peak of weight loss at 426°C and its residual char at 800°C was only 1.5%, which means ABS shows poor charring ability itself. However, when PA4T was mixed with APP, then incorporated into ABS, the initial temperature of the PA4T/APP/ABS (7.5/22.5/70) system was advanced to 342°C and the residual char of the flame-retarded composite at 800°C was improved to 11%. As known, the char residue always plays a very important role in intumescent flame-retarded system, so this is related to its good performance on the LOI test before.

Figures 5 and 6 show the experimental and calculated TG and DTG curves of PA4T/APP/ABS (7.5/22.5/70) system. The calculated curves were obtained based upon the weight percentage of the ingredients in the IFR/ABS system. As could be seen, obvious difference between the experimental and calculated curves was observed. It was found, the addition of IFR promoted decomposition of the IFR/ABS system, which caused more weight loss at 350–550°C, compared with the calculated curve (Fig. 5). However, the experimental residual char became more than the calculated one after 640°C, which was related to the thermal degradation peak found around 640°C in the calculated DTG curve disappearing in the experimental DTG curve in Figure 6. It could be deduced some high-temperature stable material was produced in the char after the former decomposition step. All above could indicate that the addition of IFR had modified the thermal degradation behavior of the IFR/ABS system.

To further understand the modification and look for the mechanism of flame-retarded action of the

TABLE III
Thermal Degradation Data Under Pure Nitrogen by TGA

Sample	T_{initial} (°C)	$R_{1\text{peak}}$ (%°C ⁻¹)	$T_{1\text{peak}}$ (°C)	$R_{2\text{peak}}$ (%°C ⁻¹)	$T_{2\text{peak}}$ (°C)	Char residue at 800°C	
						Cal.	Exp.
PA4T	439	2.6	470				7.6
APP	331	0.13	335	1.3	634		24.4
PA4TAPP (1/3)	311	0.48	358	0.23	612	20.2	27.4
ABS	394	2.3	426				1.5
PA4T/APP/ABS (7.5/22.5/70)	342	1.5	425			7	11

T_{initial} , the initial decomposition temperature (based on 5 % weight loss); $R_{1\text{peak}}$, the decomposition speed at the first decomposition peak; $T_{1\text{peak}}$, the temperature of the first decomposition peak; $R_{2\text{peak}}$, the decomposition speed at the second decomposition peak; $T_{2\text{peak}}$, the temperature of the second decomposition peak.

IFR/ABS in gaseous-phase, TG-FTIR work was carried out on the PA4T/APP (1/3) mixture. Figures 7 and 8 give the experimental and calculated TG and DTG curves of PA4T/APP (1/3) mixture, respectively. As could be seen, remarkable difference was observed between the experimental and the calculated curves of the mixture. First, the first peak of weight loss appearing at 470°C in the calculated curve was greatly advanced to 358°C in the experimental one in Figure 8. This probably means a complicated reaction between APP and PA4T had happened, which accelerated the thermal degradation of the mixture obviously at first and led to a very fast weight loss, that is, the experimental residual weight was much lower than the calculated residual weight at 310–550°C, shown in Figure 7. However, an interesting phenomenon happened. The experimental residual weight became higher than the calculated one after 650°C, such as, the residual char was improved to 27.4%, compared with the calculated one 20.2% (Table III). This is also related to the less weight loss rate around 640°C, compared with calculated DTG curve in Figure 8. It was deduced some high temperature stable char residue was

formed after the reaction between PA4T and APP to prevent the weight loss with temperature increasing.

Figure 9 gives FTIR spectra of the gaseous products during the thermal degradation of PA4T/APP(1/3) mixture under nitrogen to find more detail of the reaction between PA4T and APP, and even the mechanism of the flame-retarded action in gaseous-phase. As shown in Figure 9, when it is 250°C, there is no gaseous product observed, so this curve could be considered as baseline. When the temperature reached 300°C, typical absorptions of ammonia at 3331, 965, 930 cm⁻¹ appeared, which was mostly deriving from degradation of APP.²¹ When the temperature is 390°C, new absorption at 2935, 2865 cm⁻¹ was found, which was attributed to aliphatic hydrocarbon and deriving from degradation of PA4T. When the temperature was raised continually, absorption of aliphatic hydrocarbon disappeared, but ammonia existed all the time.

As shown in the TG-FTIR work above, it could be concluded that APP probably only destabilized PA4T without modifying the composition of the gaseous products produced during the thermal degradation of PA4T/APP (1/3) greatly, that is, ammonia

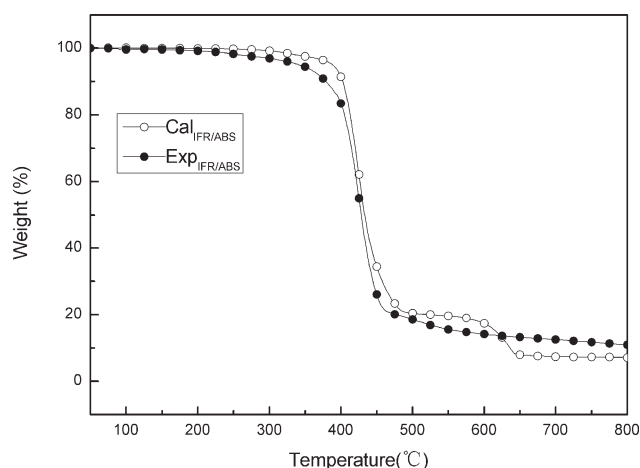


Figure 5 Experimental and calculated TG curves of IFR/ABS system.

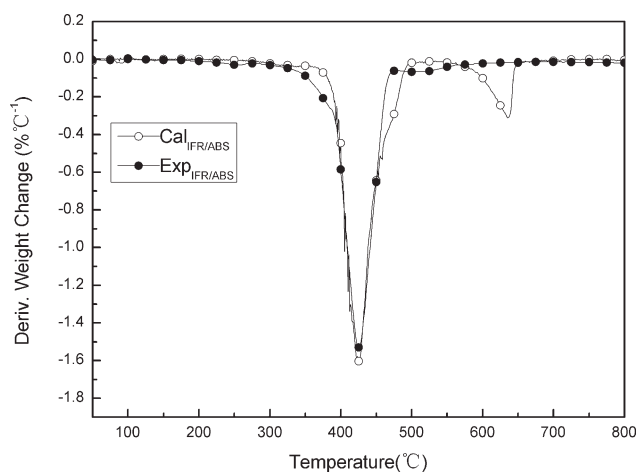


Figure 6 Experimental and calculated DTG curves of IFR/ABS system.

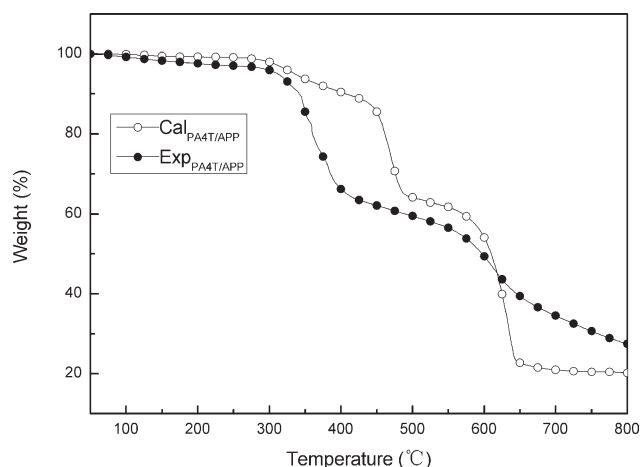


Figure 7 Experimental and calculated TG curves of PA4T/APP(1/3) mixture.

was still the main nonflammable gaseous product produced during the thermal degradation. So it is hardly to explain the fire retardant action of the PA4T/APP mixture in gaseous-phase. For this reason, solid residues formed at different temperature during the thermal decomposition of the mixture were collected and analyzed by FTIR, which is shown in Figure 10, to look for a condensed-phase mechanism of the flame retardant action. Curve a from Figure 10 shows the IR spectrum of the original mixture, absorptions typical of PA4T are evident at 1627 cm^{-1} (amide I), 1541 cm^{-1} (amide II). The peaks of $-\text{CH}_2$ ($2929, 2869\text{ cm}^{-1}$) and $-\text{NH}$ (3304 cm^{-1}) from PA4T shown in Figure 1 are overlapped with the asymmetric and symmetric stretching vibration of $-\text{NH}$ ($3198, 3061\text{ cm}^{-1}$) from APP because of ionic and hydrogen bonding. The other typical absorptions of APP are observed at 1252 cm^{-1} ($\text{P}=\text{O}$), 1077 cm^{-1} ($\text{P}-\text{O}$), 883 cm^{-1} ($\text{P}-\text{O}-\text{P}$). Curve b gives the IR spectrum of the residue collected at

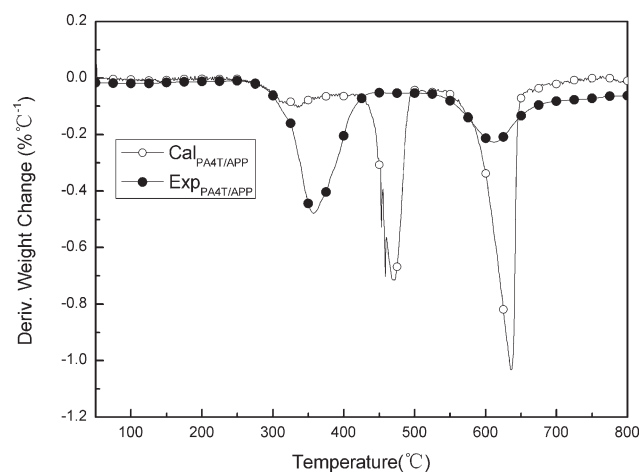


Figure 8 Experimental and calculated DTG curves of PA4T/APP(1/3) mixture.

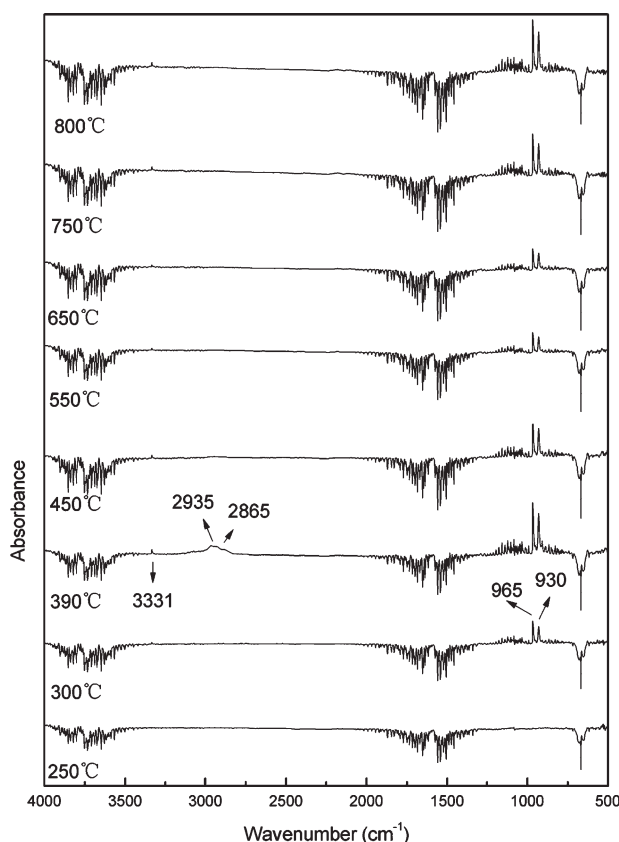


Figure 9 FTIR spectra of the gaseous products of PA4T/APP (1/3) mixture during the thermal degradation.

the end of the first weight loss step at 500°C . In comparison with the IR spectrum of the original mixture, the broad overlapping absorptions around $3000\text{--}3500\text{ cm}^{-1}$ disappear, the absorption of $-\text{CH}_2$ at $2929, 2869\text{ cm}^{-1}$ become more clear and a new strong absorption at 3438 cm^{-1} appeared, attributed to $-\text{OH}$ from $\text{P}-\text{OH}$ group, which could indicate the presence of polyphosphoric acid. Furthermore, the absorption of amide II at 1541 cm^{-1} disappear. However, new absorptions at 1230 ($\text{P}-\text{O}-\text{C}$ structure in $\text{P}-\text{C}$ complex), 1100 and 990 cm^{-1} appear, which can be attributed to phosphoric ester bonds.^{17,22} These information above could indicate the formation of alkylphosphoric esters in the first step of thermal decomposition of PA4T/APP mixture.²³

Further heating to 700°C , end of the second step of weight loss of the mixture, shown in curve c, the absorptions of $-\text{CH}_2$ group at $2800\text{--}3000\text{ cm}^{-1}$ strongly decreased and the typical absorption of APP at 1252 cm^{-1} ($\text{P}=\text{O}$) almost disappear, whereas new absorptions at $1354, 1278, 1056\text{ cm}^{-1}$ are observed. These absorptions are likely to be due to phosphorus-nitrogen containing-moiety,²⁴ which could confirm the crosslink action between PA4T and APP further. Curve d gives the IR spectrum of the solid residue at 800°C , absorptions appearing at

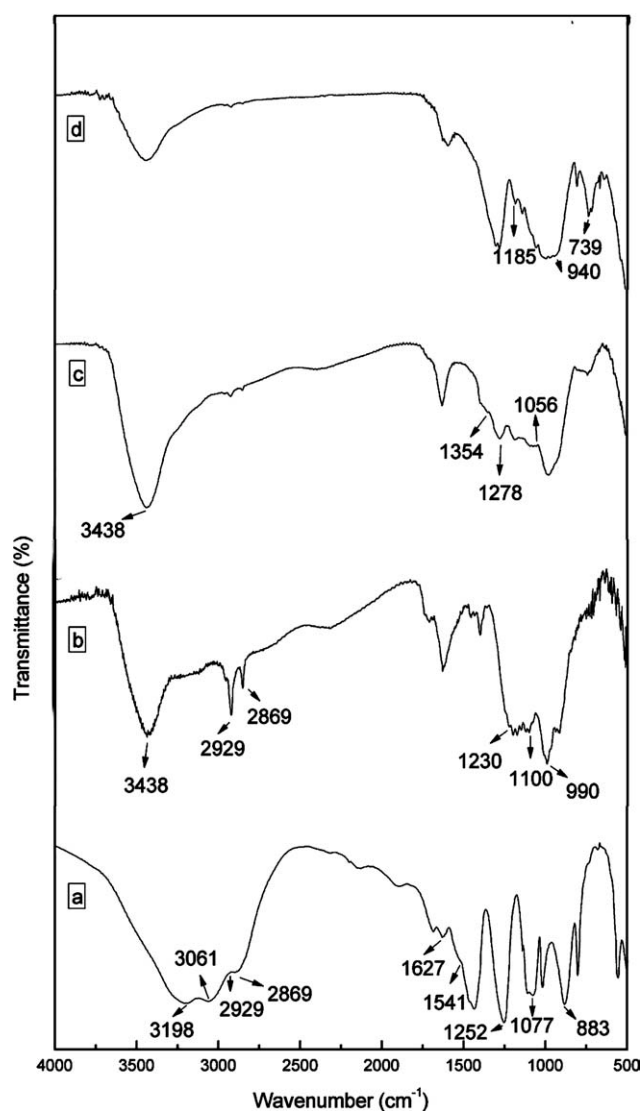


Figure 10 Infrared spectra of (a) PA4T/APP(1/3) and of solid residue (b) at 500°C (after the first step of weight loss), (c) at 700°C (after the second step of weight loss), and (d) at 800°C.

1185, 940, and 739 cm^{-1} could be attributed to a phosphorus-nitrogen crosslinked polymer of the phospham type.²⁵ At the end, according to the FTIR work above, it could be concluded some crosslinked material in condensed-phase was formed during the thermal degradation of the PA4T/APP mixture, which could make the residual char of the IFR/ABS formed during combustion more high-temperature stable and perform as a barrier between the flame and the polymeric material during combustion more effectively.

Morphology of the final char

As for the intumescent flame retardant system, it is noted that the intumescent residual char plays a very important role in improving flame retardant

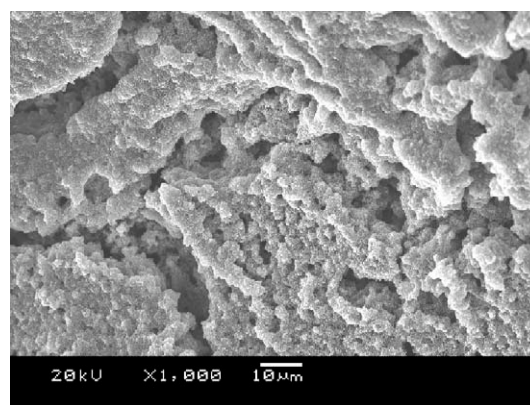


Figure 11 SEM of the residual char of APP/ABS (30/70).

behavior. Morphology of the residual char of APP/ABS(30/70) and PA4T/APP/ABS (7.5/22.5/70) formed after the LOI test was investigated by SEM, which are shown in Figures 11 and 12. It is found there are lots of big holes formed on the surface of the residual char of the APP/ABS system in Figure 11, which was closely related with its bad flame-retardant performance. However, when the intumescent flame retardant were added in ABS, a cohesive, dense cellular char layer was formed, which could effectively serve as a barrier between the flame and the polymeric material to protect underlying material, this is related to its great performance in flammability (Table I).

CONCLUSIONS

A novel intumescent flame retardant was prepared for ABS from APP (as acid source and blowing agent) and PA4T (as carbonization agent). When the weight ratio of PA4T to APP was 1 : 3, the total loading of IFR was 30%, LOI value of the IFR/ABS system reached to 30% and pass UL-94 V-1 rating. The study of thermal degradation behavior of IFR/ABS system indicated that, there was some reaction

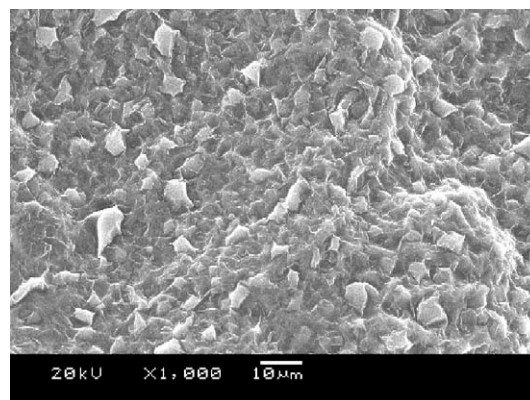


Figure 12 SEM of the residual char of PA4T/APP/ABS (7.5/22.5/70).

between PA4T and APP, resulting in the modification of thermal degradation progress of the flame-retarded ABS system and the residual char containing some high-temperature stable crosslinked material. Moreover, the morphology of the residual char obtained after combustion of PA4T/APP/ABS (7.5/22.5/70) investigated by SEM suggested that the novel IFR/ABS system can form excellent char layer, which could hinder the transfer of heat flow and combustible gas and improve the flame retardancy of ABS.

References

- Dong, D. W.; Tasaka, S.; Aikawa, S.; Kamiya, S.; Inagaki, N.; Inoue, Y. *Polym Degrad Stab* 2001, 73, 319.
- Suzuki, M.; Wilkie, C. A. *Polym Degrad Stab* 1995, 47, 217.
- Owen, S. R.; Harper, J. F. *Polym Degrad Stab* 1999, 64, 449.
- Choi, Y. S.; Xu, M. Z.; Chung, I. J. *Polymer* 2005, 46, 531.
- Wang, S. F.; Hu, Y.; Song, L.; Wang, Z. Z.; Chen, Z. Y.; Fan, W. C. *Polym Degrad Stab* 2002, 77, 423.
- Wang, S. F.; Hu, Y.; Zong, R. W.; Tang, Y.; Chen, Z. Y.; Fan, W. C. *Appl Clay Sci* 2004, 25, 49.
- Tjong, S. C.; Jiang, W. *J Appl Polym Sci* 1999, 73, 2985.
- Brebu, M.; Bhaskar, T.; Murai, K.; Muto, A.; Sakata, Y.; Uddin, M. A. *Chemosphere* 2004, 56, 433.
- Zhou, S.; Wang, Z. Z.; Gui, Z.; Hu, Y. *Fire Mater* 2008, 32, 307.
- Hornsby, P. R. *Fire Mater* 1994, 18, 269.
- Wang, J.; Tung, M. Y.; Ahmad, F.; Hornsby, P. R. *J Appl Polym Sci* 1996, 60, 1425.
- Wang, Z. Z.; Qu, B. J.; Fan, W. C.; Huang, P. *J Appl Polym Sci* 2001, 81, 206.
- Camino, G.; Delobel, R. *Fire Retardancy of Polymeric Materials*; Marcel Dekker: New York, 2000.
- Demir, H.; Arkis, E.; Balkose, D.; Uiku, S. *Polym Degrad Stab* 2005, 89, 478.
- Bras, M. L.; Bourbigot, S.; Delporte, C.; Siat, C.; Tallec, Y. L. *Fire Mater* 1996, 20, 191.
- Bras, M. L.; Bourbigot, S.; Tallec, Y. L.; Laureyns, J. *Polym Degrad Stab* 1997, 56, 11.
- Levchik, S. V.; Costa, L.; Gamino, G. *Polym Degrad Stab* 1992, 36, 229.
- Almeras, X.; Dabrowski, F.; Bras, M. L.; Poutch, F.; Bourbigot, S.; Marosi, G.; Anna, P. *Polym Degrad Stab* 2002, 77, 305.
- Zhang, Y. X.; Liu, Y.; Wang, Q. *J Appl Polym Sci* 2010, 116, 45.
- Liu, Y.; Feng, Z. Q.; Wang, Q. *Polym Compos* 2009, 30, 221.
- Herrera, M.; Matuschek, G.; Kettrup, A. *J Therm Anal Calorim* 2000, 59, 384.
- Ke, C. H.; Li, J.; Fang, K. Y.; Zhu, Q. L.; Zhu, J.; Yan, Q.; Wang, Y. Z. *Polym Degrad Stab* 2010, 95, 763.
- Levchik, S. V.; Camino, G.; Costa, L.; Levchik, G. F. *Fire Mater* 1995, 19, 1.
- Thomas, L. C. *Interpretation of the Infrared Spectra of Organophosphorus Compounds*; Heyden: London, 1974.
- Weil, E. D.; Patel, N. G. *Fire Mater* 1994, 18, 1.